Applicability of energy density formalism in describing ^{16}O+^{154}Sm, ^{186}W fusion reactions at sub-barrier energies

Muhammad Zamrun F., Takayuki Takehi, Kouichi Hagino and Noboru Takigawa
Department of Physics, Tohoku University, Sendai 980-8578, Japan

(Received 25 July 2005)

We study fusion reactions of ^{16}O with ^{154}Sm and ^{186}W at sub-barrier energies by the coupled-channels framework using the potential calculated in the energy density formalism. We use the Skyrme energy functional and estimate the kinetic energy and spin orbit densities by the extended-Thomas-Fermi method. The potential obtained in this way is then normalized so as to reproduce the experimental data of fusion excitation functions at energies around the Coulomb barrier with the calculation of one dimensional model. The renormalization partly mimics the effects of the octupole excitation of ^{16}O. We particularly analyze the fusion cross section and the fusion barrier distributions of ^{16}O with ^{154}Sm and ^{186}W reactions. In order to perform the coupled-channels calculations by taking the inelastic excitations of the colliding nuclei, i.e. the rotational excitations of ^{154}Sm and ^{186}W target nuclei, into account, we represent the potential obtained in the energy density formalism with the Woods-Saxon form. It is shown that our calculations well reproduce the experimental data of the fusion excitation functions as well as the fusion barrier distributions of these reactions.

I. INTRODUCTION

Heavy-ion fusion reactions at energies near and below the Coulomb barrier have been extensively studied over the last two decades. These studies were motivated by the discovery that the cross-sections of heavy-ion fusion reactions with medium weight nuclei at energies below the Coulomb barrier are several of magnitude larger than the prediction of a potential model calculation [1]. It is now well known that this enhancement can be attributed to the coupling of translational motion to additional degrees of freedom such as nuclear surface vibration, deformation, rotation, nucleon transfer and neck formation [2,3]. A standard approach to address the effect of nuclear intrinsic degrees of freedom is to numerically solve the coupled channels equations by including dominant nuclear intrinsic excitations as well as transfer reactions.

A large number of precision data of the fusion cross-section allow detailed studies of the effect of nuclear intrinsic degrees of freedom through the analysis of the so-called fusion barrier distributions [3]. In interpreting these data, both simplified [4,5], and realistic [6,7], coupled-channels codes have been used. In most analysis of the data, phenomenological Woods-Saxon potential has been assumed for the nuclear potential, and the depth, range and surface diffuseness parameters have been determined to fit the experimental fusion excitation function at high energies. Instead of such phenomenological approach, here we perform the coupled-channels calculations based on the potential given by the energy density formalism. The aim of this study is to see weather this approach, which is parameter free like double folding model [8], works to explain the fusion data of ^{16}O+^{154}Sm,^{186}W reactions by taking the rotational excitations of target nuclei into account.

II. ION-ION POTENTIAL IN ENERGY DENSITY FORMALISM

In the frozen density approximation, the interaction potential between two colliding ions can be written as [9] (see Fig. 1 for definition of the coordinates)

$$V_{\rm nuc}(R) = \int \varepsilon_{\rm nuc}[\rho_{\rm P+T}(\vec{r};\vec{R})]d\vec{r} - \int \varepsilon_{\rm nuc}[\rho_{\rm T}(\vec{r}_{\rm T})]d\vec{r}_{\rm T} - \int \varepsilon_{\rm nuc}[\rho_{\rm P}(\vec{r}_{\rm P})]d\vec{r}_{\rm P} \quad (1)$$

where ε is the energy density and ρ is density. The first term is the total energy of combined system where its density is assumed to be given as $\rho_{\rm P+T}(\vec{r};\vec{R}) = \rho_{\rm P}(\vec{r}) + \rho_{\rm T}(\vec{r}-\vec{R})$. The second and the third terms are the total energy of target and projectile nuclei, respectively.

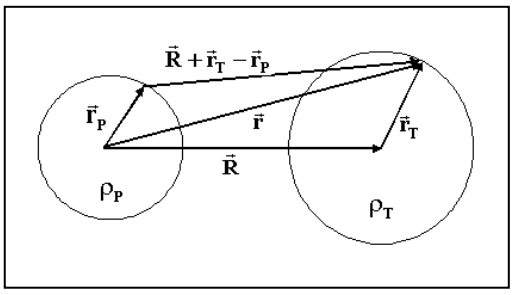

FIG. 1. Definition of target (T) and projectile (P) coordinates.

The energy density functional associated with the Skyrme interaction is given by

$$\begin{aligned}\varepsilon_{\text{nuc}}(\vec{r}) = {} & \frac{\hbar^2}{2m}\tau + \frac{t_0}{2}\left(1+\frac{x_0}{2}\right)\rho^2 - \frac{t_0}{2}\left(x_0+\frac{1}{2}\right)\left(\rho_p^2+\rho_n^2\right) + \frac{1}{4}\left[t_1\left(1+\frac{x_1}{2}\right)+t_2\left(1+\frac{x_2}{2}\right)\right]\rho\tau \\ & - \frac{1}{4}\left[t_1\left(x_1+\frac{1}{2}\right)-t_2\left(x_2+\frac{1}{2}\right)\right]\left(\rho_n\tau_n+\rho_p\tau_p\right) + \frac{1}{16}\left[3t_1\left(1+\frac{x_1}{2}\right)-t_2\left(1+\frac{x_2}{2}\right)\right]\left(\nabla\rho\right)^2 \\ & - \frac{1}{16}\left[3t_1\left(x_1+\frac{1}{2}\right)+t_2\left(x_2+\frac{1}{2}\right)\right]\left[\left(\nabla\rho_p\right)^2+\left(\nabla\rho_n\right)^2\right] \\ & + \rho^\alpha\left[\frac{t_3}{12}\left(1+\frac{x_3}{2}\right)\rho^2 - \frac{t_3}{12}\left(x_3+\frac{1}{2}\right)\left(\rho_p^2+\rho_n^2\right)\right] + \frac{W_0}{2}\left[\vec{J}\bullet\nabla\rho + \vec{J}_p\bullet\nabla\rho_p + \vec{J}_n\bullet\nabla\rho_n\right]\end{aligned} \tag{2}$$

The kinetic energy, τ_q and spin orbit, $\vec{J}_q$ densities, where $q=(p,n)$, are approximated with semi-classical extended Thomas-Fermi model [10] up to second order correction in the power of $\hbar$. The kinetic energy density takes the form

$$\begin{aligned}\tau_q[\rho_q] = {} & \frac{3}{5}(3\pi^2)^{2/3}\rho_q^{5/3} + \frac{(\nabla\rho_q)^2}{36\rho_q} + \frac{\nabla^2\rho_q}{3} + \frac{\nabla\rho_q\bullet\nabla f_q}{6\rho_q} \\ & + \frac{\rho_q\nabla^2 f_q}{6f_q} - \frac{\rho_q(\nabla f_q)^2}{12 f_q^2} + \left(\frac{2m}{\hbar^2}\right)^2\frac{\rho_q}{2}\left(\frac{\vec{W}_q}{f_q}\right)^2.\end{aligned} \tag{3}$$

Here the effective-mass form factor is given by

$$\begin{aligned}f_q(\vec{r}) = 1 + \frac{m}{2\hbar^2}\Bigg\{ & \left[t_1\left(1+\frac{x_1}{2}\right)+t_2\left(1+\frac{x_2}{2}\right)\right]\rho(\vec{r}) \\ & - \left[t_1\left(x_1+\frac{1}{2}\right)-t_2\left(x_2+\frac{1}{2}\right)\right]\rho_q(\vec{r})\Bigg\}.\end{aligned} \tag{4}$$

The spin-orbit potential the spin orbit density are given as

$$\vec{W}_q(\vec{r}) = \frac{W_0}{2}\nabla\left[\rho(\vec{r})+\rho_q(\vec{r})\right] \tag{5}$$

$$\vec{J}_q = -\frac{2m}{\hbar^2}\frac{\rho_q}{f_q}\vec{W}_q. \tag{6}$$

The Coulomb interaction between two colliding ions is determined by

$$\begin{aligned}V_{\text{C}}(R) = {} & \int\frac{\rho_{p(\text{P})}(\vec{r}_{\text{P}})\rho_{p(\text{T})}(\vec{r}_{\text{T}})}{\left|\vec{R}+\vec{r}_T-\vec{r}_P\right|}\,d\vec{r}_{\text{P}}d\vec{r}_{\text{T}} \\ & - \frac{3e^2}{4}\left(\frac{3}{\pi}\right)^{1/3}\Bigg\{\int\left[\rho_{p(\text{P})}(\vec{r}_{\text{P}})+\rho_{p(\text{T})}(\vec{r}-\vec{R})\right]^{4/3}d\vec{r} \\ & - \int\left[\rho_{p(\text{P})}(\vec{r}_{\text{P}})\right]^{4/3}d\vec{r}_{\text{P}} - \int\left[\rho_{p(\text{T})}(\vec{r}_{\text{T}})\right]^{4/3}d\vec{r}_{\text{T}}\Bigg\}\end{aligned} \tag{7}$$

for the direct term and the exchange contribution. The total s-wave scattering potential is then given by the sum of Eq. (1) and Eq. (7).

III. RESULTS AND FURTHER DEVELOPMENT

In performing the calculation of Eqs. (1) and (7), we use SkM* parameter set [11]. The proton and neutron distributions of the target and projectile nuclei which we considered was approximated by modified Fermi shape

$$\rho_q(r) = \rho_{0q}[1+\exp\{(r-R_{0q})/a_q\}]^{\gamma_q} \tag{8}$$

where the parameters ρ_{0q}, R_{0q}, a_q and γ_q are adjusted in order to reproduce the corresponding proton and neutron densities of of SkM*-Hartree-Fock calculations.

The resulting potentials are then used in the calculation of the fusion cross section and the fusion barrier distribution in one-dimensional barrier penetration model of the fusion reactions which we are interested in. The potentials are normalize in order to reproduce the experimental data of fusion excitation function around the Coulomb barrier in these calculations. The normalization is partly mimics the effect of 3^- state of ^{16}O projectile. The results are given by the dashed lines in the Figs. 2 and 3. However, it significantly underestimates the fusion cross section at low energies. Also, the experimental fusion barrier distribution is much broader than the prediction of the single channel model. It is known that these phenomena

are caused by the coupling of the relative motion between the projectile and target nuclei to their shape as well as to their collective excitations.

In order to perform the coupled channels calculation by taken into account the rotational excitation of ^{154}Sm and ^{186}W target nuclei, we fit the normalized potential obtained in the one dimensional model by Woods-Saxon form. The optimum Woods-Saxon potential parameters are V_0 = 82.36 MeV, R_0 = 1.144 fm and a = 0.75 fm for ^{16}O+^{154}Sm reaction and V_0 = 86.86 MeV, R_0 = 1.152 fm and a = 0.73 fm for ^{16}O+^{186}W reaction. In performing the numerical coupled-channels calculation of the fusion excitation function and the fusion barrier distribution, we used CCFULL code [7].

Fig. 2 then compares the experimental data with the coupled-channels calculations of the excitation function of the fusion cross-section (left panel) and the fusion barrier distribution (right panel) for the ^{16}O+^{154}Sm system. We include the deformation parameter up-to β_6 of ^{154}Sm and its ground state rotational band up-to I_{max} = 10^+ member. The huge enhancement of the fusion cross section and the fusion barrier distribution can be explained in this way. We adjusted the values of the deformation parameters to fit the experimental fusion cross section at energies below the Coulomb barrier. The resultant values are: β_2 = 0.33, β_4 = 0.07 and β_6 = –0.015. Our optimum deformations parameters agree with the values obtained from proton scattering experiment, [13]. We apply the same procedure to ^{16}O+^{186}W fusion reactions and take the ground state rotational band of ^{186}W up-to the 14^+ member into account. The results are shown in Fig. 3. Similarly to the ^{16}O+^{154}Sm fusion reaction, the coupled channels calculations well reproduce the experimental data of the fusion cross-section as well as the fusion barrier distribution. The deformation parameters obtained to be β_2 = 0.335, β_4 = –0.045 and β_6 = 0.018. These values well agree with the analysis of the data of neutron scattering by Delaroche [14].

It is an interesting future subject to perform the full-order coupled-channels calculations with the genuine energy density formalism to explore the connection between the saturation property, which is incorporated in this formalism, and the steep fall-off problem [15] which recently was observed in the ^{64}Ni + ^{64} Ni fusion reaction.

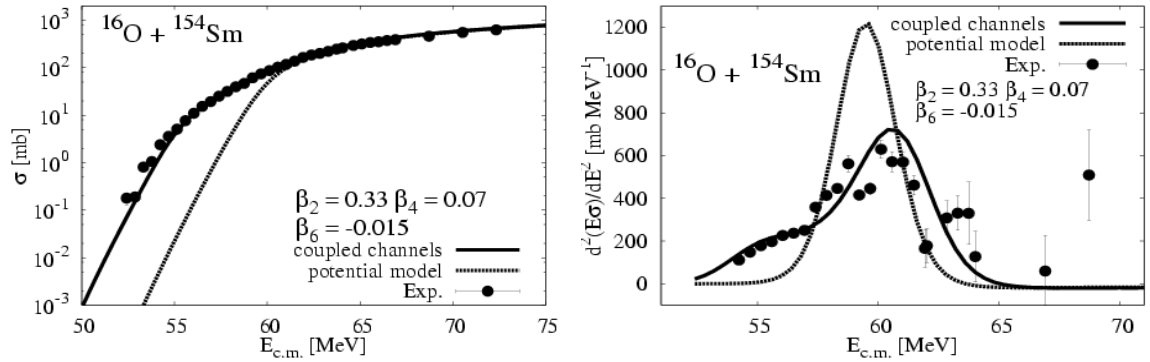

FIG. 2. Comparison of theoretical fusion excitation function (left) and fusion barrier distribution (right) with experimental data [12]. The solid line obtained with coupled channels calculations by including the rotational excitation of target nucleus while the dashed line represent the potential model results for ^{16}O+^{154}Sm reaction.

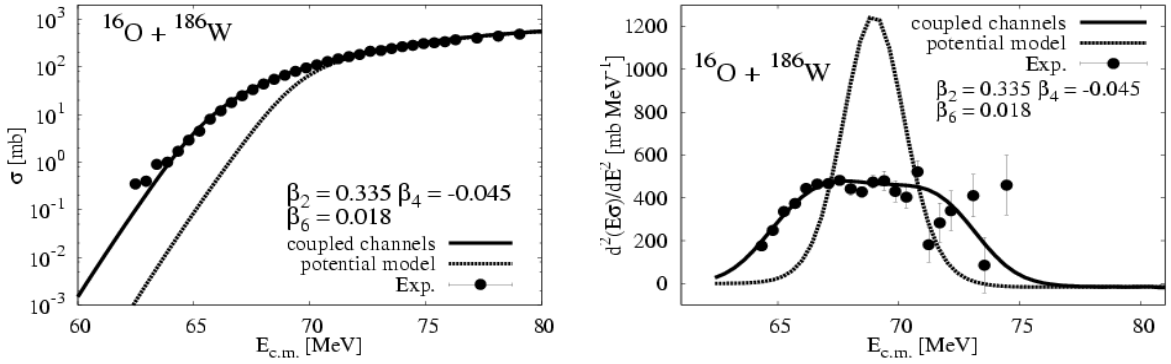

FIG. 3. The same as Fig. 4.1 but for ^{16}O+^{186}W reaction.

REFERENCES

[1] M. Beckerman, Rep. Prog. Phys., **51**, 1047 (1988).
[2] A. B. Balantekin and N. Takigawa, Rev. Mod. Phys., **70**, 77 (1998).
[3] M. Dasgupta *et al*., Annu. Rev. Part. Sci., **48**, 401 (1998).
[4] C. H. Daso and S. Landowne, Comput. Phys. Commun., **46**, 187 (1991).
[5] J. Fernandes-Nielo *et al.*, Comput. Phys. Commun., **54**, 409 (1987).
[6] I. J. Thompson, Comput. Phys. Rep., **7**, 167 (1988).
[7] K. Hagino, N. Rowley and A. T. Kruppa, Comput. Phys. Commun., **123**, 143 (1999).
[8] G. R. Satchler and W. G. Lowe, Physics Reports, **55**, 183 (1979).
[9] A. Dobrowolski, K. Pomorski and J. Bartel, Nucl. Phys. A, **729**, 713 (2003).
[10] M. Brack, C. Guet and H. B. Hakansson, Phys. Rep., **123**, 275 (1985).
[11] J. Bartel, P. Quentin, M. Brack, C. Guet and H. B. Hakansson, Nucl. Phys. A**, 386**, 79 (1982).
[12] J. R. Leigh *et al*., Phys. Rev. C, **52**, 3151 (1995).
[13] G. Palla, H. V. Geramb and C. Pegel, Nucl. Phys. A, **403**, 134 (1983).
[14] J. P. Delaroche, Phys. Rev. C, **26**, 1899 (1982).
[15] C. L. Jiang *et al*., Prog. Theor. Phys. Suppl., **154**, 61 (2004).